

# On the theory of condensin mediated loop extrusion in genomes

Ryota Takaki,<sup>1</sup> Atreya Dey,<sup>2</sup> Guang Shi,<sup>2</sup> and D. Thirumalai<sup>2,\*</sup>

<sup>1</sup>*Physics Department, The university of Texas at Austin*

<sup>2</sup>*Chemistry Department, The university of Texas at Austin*

(Dated: January 20, 2022)

The condensation of several mega base pair human chromosomes in a small cell volume is a spectacular phenomenon in biology. This process, involving the formation of loops in chromosomes, is facilitated by ATP consuming motors (condensin and cohesin), that interact with chromatin segments thereby actively extruding loops. Motivated by real time videos of loop extrusion (LE), we created an analytically solvable model, which yields the LE velocity as a function of external load acting on condensin. The theory fits the experimental data quantitatively, and suggests that condensin must undergo a large conformational change, triggered by ATP binding and hydrolysis, that brings distant parts of the motor to proximity. Simulations using a simple model confirm that a transition between an open and closed states is necessary for LE. Changes in the orientation of the motor domain are transmitted over  $\sim 50$  nm, connecting the motor head and the hinge, thus providing a plausible mechanism for LE. The theory and simulations are applicable to loop extrusion in other structural maintenance complexes.

How chromosomes are structurally organized in the tight cellular space is a long standing problem in biology. Remarkably, these information carrying polymers in humans containing more than 100 million base pairs, depending on the chromosome number, are densely packed (apparently with negligible knots) in the  $5 - 10 \mu\text{m}$  cell nucleus [1, 2]. In order to accomplish this herculean feat nature has evolved a family of SMCs (Structural Maintenance of Chromosomes) complexes [3, 4] (bacterial SMC, cohesin, and condensin) to facilitate large scale compaction of chromosomes in all living systems. Compaction is thought to occur by active generation of a large array of loops, which are envisioned to form by extrusion of the genomic material [5, 6] driven by ATP-consuming motors. The SMC complexes have been identified as a major component of the loop extrusion (LE) process [3, 4].

Of interest here is condensin, which has motor activity as it translocates on DNA [7], resulting in active extrusion loops in an ATP-dependent manner [8]. We first provide a brief description of the architecture of condensin (drawn schematically in Fig.1) because the theory is based on this picture. Condensin is a ring shaped dimeric motor to which a pair of SMC proteins (Smc2 and Smc4) are attached. Smc2 and Smc4, which have coiled coil (CC) structures, are connected at the hinge domain. The ATP binding domains are in the motor heads [4, 9]. The CCs have kinks roughly in the middle of the CCs [9]. The relative flexibility in the elbow region (located near the kinks) could be the key to the conformational transitions in the CC that are powered by ATP binding and hydrolysis [4, 10]. At present, there is no direct experimental evidence that this is so.

Previous studies using simulations [6, 11, 12], which build on the pioneering insights by Nasmyth [5], suggested that multiple condensins concertedly translocate

along the chromosome extruding loops of increasing length. In this mechanism two condensin heads move away from each other extruding loops in a symmetric manner. Cooperative action of many condensins [13, 14] might be necessary to account for the  $\sim (1,000 - 10,000)$  fold compaction of human chromosomes [15]. In the only available theoretical study thus far [16], a plausible catalytic cycle for the condensin is coupled to loop extrusion. The present theory may be viewed as complementary to the earlier study but differs not only in details but also in the envisioned LE mechanism.

We were inspired by a real time video of LE in  $\lambda$ -DNA by a single condensin [8], which functions by extruding loops through one head while the other head is likely fixed. To describe the experimental outcomes quantitatively, we created an analytically solvable model that produces excellent agreement with experiments for the LE velocity as a function of external load. The theory suggests that in order for LE to occur there has to be ATP-powered allosteric transition in condensin involving a large conformational change that brings distant parts of the motor to proximity. Simulations using a simple model confirmed this finding, and further strongly suggest that the conformational transitions are driven by a scrunching mechanism, discovered in the context of transcription initiation by RNA polymerase resulting in bubble formation in promoter DNA [17], and further illustrated in molecular simulations [18].

In order to develop a model applicable to condensin (and cohesin), we assume that condensin is attached to two loci (**A** and **B**) on the DNA. To retain the generality of the theory, we do not explicitly describe the nature of the attachment points at this juncture. However, the picture in Fig.1 could be mapped onto a couple of working models proposed in the literature. In the scrunching model [19] the blue (red) sphere would be the motor heads (hinge). In the so-called pumping model [16], location **A** might correspond to the two heads of SMC complex, which trap one end of the DNA. The red sphere

\* dave.thirumalai@gmail.com

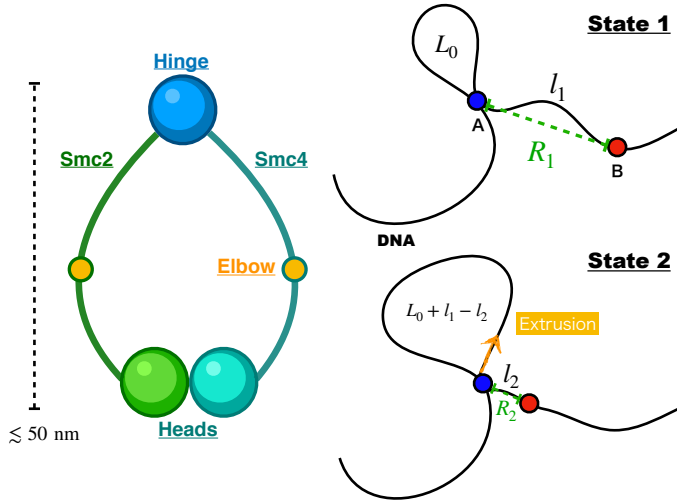


FIG. 1. **Left panel:** Caricature of the structure of condensin, which has two heads (ATPase domains) and a hinge connected by coiled-coils, labeled Smc2 and Smc4. In the middle of the CCs there is a flexible kink, referred to as an elbow. **Right panel:** A schematic of the physical picture for one-sided loop extrusion based on the architecture of a generic SMC complex. DNA is attached to two structural regions on condensin. In state 1 (upper panel) the conformation of condensin is extended with the spatial distance between **A** and **B** equal to  $R_1$ . The genomic length at the start is  $L_0$ , which can be large or small. After the conformational transition (state 1 to state 2) the distance between **A** and **B** shrinks to  $R_2$ , and the length of the extrusion during the single transition is  $\Delta l = l_1 - l_2$ , which would vary from cycle to cycle.

in Fig.1 would be localized on the coiled coil to which the genome is transiently attached. In state 1, the spatial distance between the condensin attachment points is,  $\mathcal{R} = R_1$  (Fig.1), and the genomic length between **A** and **B** is  $l_1$ . Due to the polymeric nature of the DNA, the captured length  $l_1$  can exceed  $R_1$ . However,  $R_1$  cannot be greater than the overall dimension of the SMC motor, which is on the order of  $\sim 50$  nm. Once a loop in the DNA is captured, condensin undergoes a conformational change triggered by either ATP binding and/or ATP hydrolysis, shrinking the distance from  $R_1$  to  $R_2$  (where  $R_2 < R_1$ ). As a result, the captured genomic length between **A** and **B** reduces to  $l_2$  (state 2). Consequently, the loop grows by  $l_1 - l_2$ . We define the step size of condensin as  $\Delta R = R_1 - R_2$ , and extrusion length per step is  $\Delta l = l_1 - l_2$ .

In order to derive the velocity of loop extrusion, we first estimate the loop length of DNA  $\mathcal{L}$  captured by condensin when the attachment points are spatially separated by  $\mathcal{R}$ . We show that on the length scale of the size of condensin ( $\sim 50$  nm), it is reasonable to approximate  $\mathcal{L} \approx \mathcal{R}$ . To calculate the LE velocity it is necessary to estimate the total work done to bend the DNA as well as account for the work associated when an external load is applied [8]. Based on these considerations, we derive an expression for the LE velocity, given by  $k_0 \exp(-f\Delta R/k_B T)\Delta R$ ,

where  $k_0$  is the rate of mechanical step at zero load,  $f$  is the external load,  $k_B$  is Boltzmann constant and  $T$  is temperature.

We examined the possibility that the loop extrusion length per step can be considerably larger than the size of condensin [7–9, 20] by calculating,  $P(\mathcal{L}|\mathcal{R})$ , the conditional probability that for realizing the contour length  $\mathcal{L}$  for a given end-to-end distance,  $\mathcal{R}$ . An exact expression for the radial distance of end-to-end probability for a fixed contour length ( $P(\mathcal{R}|\mathcal{L})$ ) for a semi-flexible polymer has been derived [21] but it is complicated. We have calculated  $P(\mathcal{R}|\mathcal{L})$  using a mean-field theory that gives excellent approximation [22, 23] to the exact expression, which suffices for our purposes here. The expression for  $P(\mathcal{L}|\mathcal{R})$ , which has the same form as  $P(\mathcal{R}|\mathcal{L})$  up to a normalization constant, is given by, (Supplementary Information),

$$P(\mathcal{L}|\mathcal{R}) = C \frac{4\pi N\{\mathcal{L}\}(\mathcal{R}/\mathcal{L})^2}{\mathcal{L}(1 - (\mathcal{R}/\mathcal{L})^2)^{9/2}} \exp\left(-\frac{3t\{\mathcal{L}\}}{4(1 - (\mathcal{R}/\mathcal{L})^2)}\right), \quad (1)$$

where  $t\{\mathcal{L}\} = 3\mathcal{L}/2l_p$ ,  $l_p$  is the persistence length of the polymer, and  $N\{\mathcal{L}\} = \frac{4\alpha^{3/2}e^\alpha}{\pi^{3/2}(4+12\alpha^{-1}+15\alpha^{-2})}$  with  $\alpha\{\mathcal{L}\} = 3t/4$ . In Eq.(1),  $C$  is a normalization constant that does not depend on  $\mathcal{L}$ . The distribution  $P(\mathcal{L}|\mathcal{R})$ , which scales as  $\mathcal{L}^{-3/2}$  for large  $\mathcal{L}$ , has a heavy tail and does not have a well defined mean (see Fig. 2a for the plots of  $P(\mathcal{L}|\mathcal{R})$  for different  $\mathcal{R}$ ). Therefore, we evaluated the location of the peak ( $\mathcal{L}_{peak}$ ) in  $P(\mathcal{L}|\mathcal{R})$ , and solved the resulting equation numerically. The dependence of  $\mathcal{L}_{peak}$  on  $\mathcal{R}$ , which is almost linear (Fig.2b), is well fit using  $\mathcal{L}_{peak} = \mathcal{R} \exp(a\mathcal{R})$  with  $a = 0.003 \text{ nm}^{-1}$  at the length scale  $\mathcal{R} < 60 \text{ nm}$ . Therefore, with negligible corrections, we used the approximation  $\mathcal{L} \approx \mathcal{R}$  on the length scales corresponding to the size of condensin or the DNA persistence length. Note that the probability that  $P(\mathcal{L}|\mathcal{R})$ , for a given  $l_p$  ( $= 50 \text{ nm}$  in Fig.2), is small for large  $\mathcal{L}$ . Indeed, the location of the largest probability is at  $\mathcal{L} \approx l_p \approx \mathcal{R}$ , which is similar to what was found for proteins as well [24]. Furthermore, the presence of an external load would stretch the DNA, further justifying the assumption ( $\mathcal{L} \approx \mathcal{R}$ ). Thus, LE of DNA loop that is much larger than the size of condensin is unlikely, at least as the principal mechanism. This suggests that the step size of condensin is nearly equal to the extrusion length of DNA,  $\Delta R \approx \Delta l$ .

Just like other motors, condensin hydrolyzes ATP, generating  $\mu \approx 20 \text{ } k_B T$  chemical energy that is converted into mechanical work, which in this case results in extrusion of DNA loop [8]. To arrive at an expression for LE velocity, we calculated the thermodynamic work required for LE. The required work  $W$  modulates the rate of mechanical process by the exponential factor  $\exp(-W/k_B T)$ . In our model,  $W$  has two contributions. The first is the work needed ( $W_{bend}$ ) to bend the DNA. Condensin bends the DNA by decreasing the spatial distance between the attachment points from  $\mathcal{R} = R_1$

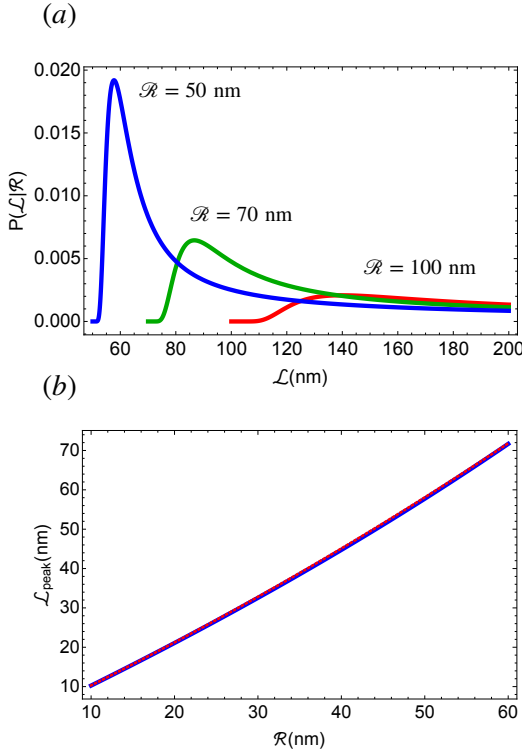


FIG. 2. (a)  $P(L|R)$  for different  $R$ .  $R = 40$  nm (in red),  $R = 50$  nm (in blue), and  $R = 60$  nm (in green). (b) Position of the peak for  $P(L|R)$ , denoted as  $L_{peak}$ , as a function of  $R$ . Blue line is the numerically evaluated peak obtained by  $dP(L|R)/dL = 0$ . The dotted red line is the fit,  $L_{peak} = R \exp(aR)$  with  $a = 0.003 \text{ nm}^{-1}$ . We used  $l_p^{DNA} = 50 \text{ nm}$  as the persistence of DNA.

to  $R = R_2$  (Fig.1). The associated genomic length of DNA in this process is  $L_\Sigma = L_0 + l_1$  (Fig.1). Note that  $L_0$  could be large or small. The second contribution is  $W_{step}$ , which comes from application of an externally applied load ( $f$ ). Condensin resists  $f$  up to a threshold value [8]. The mechanical work done during the step size  $\Delta R = R_1 - R_2$  is  $W_{step} = f\Delta R$ .

We calculated  $W_{bend}$  as the free energy change for bringing a semi-flexible polymer with contour length  $L_\Sigma$ , from the end-to-end distance  $R_1$  to  $R_2$ . It can be estimated using the relation,  $W_{bend} \approx -k_B T \log(P(R_2|L_\Sigma)) + k_B T \log(P(R_1|L_\Sigma))$ , where  $P(R|L)$  is given by Eq.(1) without the factor  $C$ . Although  $P(R|L)$  is a distribution, implying that there is a distribution for  $W_{bend}$ , for illustrative purposes, we plot  $W_{bend}$  for a fixed  $R_1 = 50$  nm at different values of  $R_2$  in Fig.3. It is evident that condensin has to overcome the highest bending penalty in the first step of extrusion, and subsequently  $W_{bend}$  is flat. If  $R_1 = 50$  nm, which is approximately the size of condensin, we estimate that condensin pays  $3 k_B T$  to initiate the extrusion process (blue line in Fig.3).

Once the energetic costs for LE are known, we can calculate the LE velocity as a function of an external load

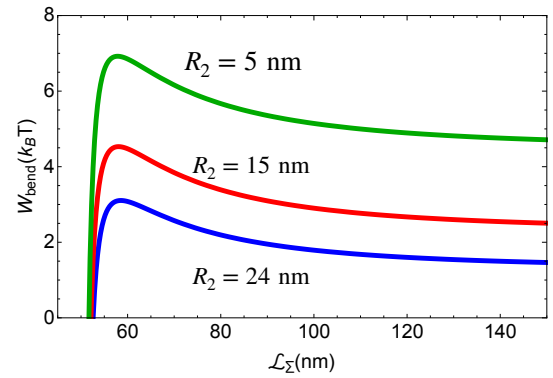


FIG. 3. Energetic cost to bend DNA,  $W_{bend}$ , as a function of  $L_\Sigma$ .  $L_\Sigma$  is the sum of the length of DNA that is already extruded ( $L_0$ ) and the length newly captured ( $l_1$ ). Note that  $L_\Sigma \geq R_1$  by physical consideration. We set  $R_1 = 50 \text{ nm}$  which is the size of condensin.  $R_2 = 24 \text{ nm}$ ,  $15 \text{ nm}$ , and  $5 \text{ nm}$  for blue line, red line, and green line, respectively.

applied to condensin. From energy conservation, we obtain the equality,  $n\mu = W_{bend} + W_{step}\{f\} + Q$ , where  $n$  is the number of ATP molecules consumed per mechanical step,  $\mu$  is the energy released by ATP hydrolysis, and  $Q$  is the heat dissipated during the extrusion process. The maximum force is obtained when the equality  $n\mu = W_{bend} + W_{step}\{f_{max}\}$  holds. If we denote the rate of mechanical transition as  $k^+$  and reverse rate as  $k^-$ , fluctuation theorem [25–27] with conservation of energy gives the following relation:

$$k^+ / k^- = e^{(n\mu - (W_{bend} + W_{step}\{f\})) / k_B T}. \quad (2)$$

Once the details of the catalytic cycle of the SMC motor are identified it is possible to extend Eq.(2) to multiple intermediate steps to include ATP dependence, ([27] for theoretical descriptions in the context of molecular machines). We can extract the load dependent term in the expression, which is written as,

$$k^+ = k_0 e^{-W_{step}\{f\} / k_B T}, \quad (3)$$

where  $k_0 = k^- e^{(n\mu - W_{bend}) / k_B T}$  is the rate of the mechanical transition at 0 load. Thus, with the assumption that  $\Delta R$  is the extruded length per reaction cycle, the velocity of LE,  $\Omega$ , may be written as,

$$\Omega\{f\} = k_0 e^{-f\Delta R / k_B T} \Delta R. \quad (4)$$

In the experimental set up in Ganji et al. [8]  $f$  is related to the relative DNA extension, which can be calculated using the expression [28, 29],

$$f = \frac{k_B T}{2l_p} \left[ 2\chi + \frac{1}{2} \left( \frac{1}{1-\chi} \right)^2 - \frac{1}{2} \right], \quad (5)$$

$\chi = R/L$ , where  $R$  is end-to-end distance of the whole DNA and  $L$  is the contour length.

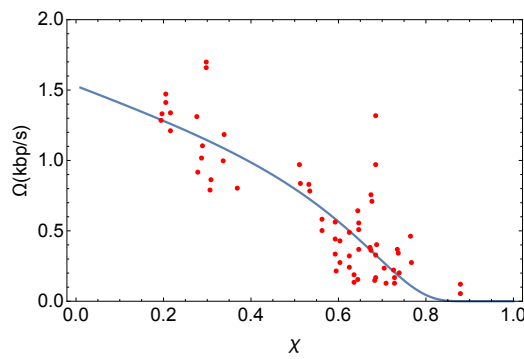


FIG. 4. The velocity of loop extrusion by condensin as a function of the relative extension of the DNA ( $\chi$ ). Red dots are from the experiment [8], and the solid line is the theoretical fit. The fitting parameters are  $k_0 = 20 \text{ s}^{-1}$  and  $\Delta R = 26 \text{ nm}$ . We used  $l_p^{DNA} = 50 \text{ nm}$  for the persistence length of the DNA. The velocity (in unit of  $\text{nm/s}$ ) may be obtained using the conversion  $1 \text{ bps} = 0.34 \text{ nm}$ .

We used Eq.(4) to fit the experimentally measured LE velocity as a function of DNA extension [8]. The fitting parameters are  $\Delta R$ , and  $k_0$ , the step size for condensin, and the rate of extrusion at 0 load, respectively. In principle,  $\Delta R$  could be determined experimentally once the structures of motors in different nucleotide binding states are known. For now, excellent fit of theory to experiments, especially considering the dispersion in the data, gives  $k_0 = 20 \text{ s}^{-1}$  and  $\Delta R = 26 \text{ nm}$ . This indicates that condensin undergoes a conformational change, with  $\Delta R \sim 26 \text{ nm}$ , during each extrusion cycle. We note that  $k_0 = 20 \text{ s}^{-1}$  is one order of magnitude faster than the hydrolysis rate estimated from experiments,  $2 \text{ s}^{-1}$  [7, 8]. The value of  $k_0$  obtained here is the same as was the value assume elsewhere [16], who also obtained an expression for LE velocity as a function. The shape of the curve in [16] is similar to the one calculated using our theory.

Next we tested whether the predicted value of  $\Delta R \sim 26 \text{ nm}$  is reasonable using simulations of a simple model. Because the ATPase domains are located at the heads of condensin, it is natural to assume that the head domain undergoes conformational transitions upon ATP binding and/or hydrolysis. The structure of prokaryotic SMC suggests that there is a change in the angle between the two heads upon ATP binding [9]. Furthermore, images of the CCs of the yeast condensin (Smc2-Smc4) using liquid atomic force microscopy (AFM) show they could adopt a few distinct shapes [19, 30]. Based on these experiments, we hypothesize that the conformational changes initiated at the head domain results in changes in the angle at the junction connecting the motor head to the CC that propagates through the whole condensin via the CC by an allosteric mechanism. The open (O-shaped in [9]), with the hinge that is  $\approx 45 \text{ nm}$  away from the motor domain, and the closed (B-shaped in Fig.1 in [9] in which the hinge domain is in proximity to the motor domain) are the two relevant allosteric states for LE. To capture

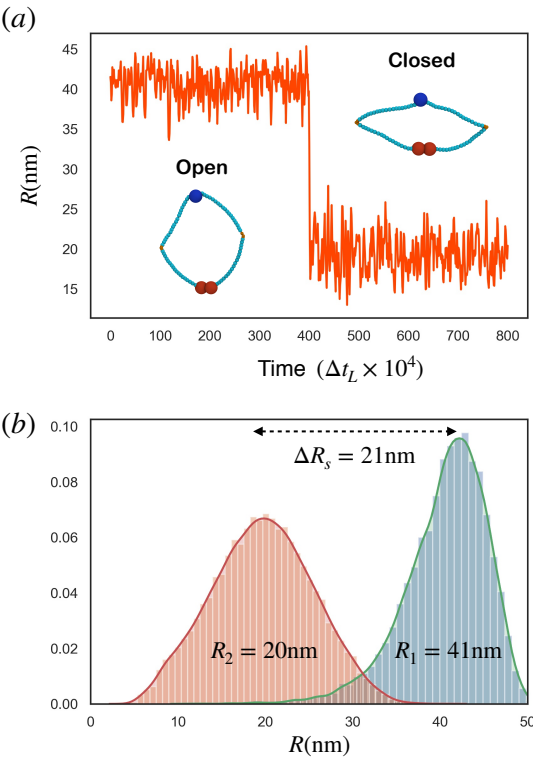


FIG. 5. Simulations for the transition between O  $\rightarrow$  B transition. (a) Example of a trajectory showing the change in the head-hinge distance  $R$ . The trajectory is for  $l_p^{CC} \sim 70 \text{ nm}$ .  $\Delta t_L$  is the time step of simulation (SI) (b) Distributions of  $P(R_1)$  and  $P(R_2)$  with  $l_p^{CC} \sim 70 \text{ nm}$ . The histogram for open state and closed state are in blue and red, respectively. The mean values of open state and closed state ( $R_1 = 41 \text{ nm}$  and  $R_2 = 20 \text{ nm}$ , respectively) are indicated in the figure. The distributions were calculated from 50 trajectories (40,000 time points).

the reaction cycle (O  $\rightarrow$  B  $\rightarrow$  O), we model the CCs as kinked semi-flexible polymers (two moderately stiff segments connected by a flexible elbow), generalizing a similar description of stepping of Myosin V on actin [31]. By altering the angle between the two heads the allosteric transition between the open (O-shaped) and closed (B-shaped) states could be simulated (SI contains the details).

We tracked the head-hinge distance in open state ( $R_1$ ) and closed state ( $R_2$ ), and  $\Delta R_s = R_1 - R_2$ , in the simulations. The sample trajectory in Fig.5a, monitoring the conformational transition between the open and closed states, shows that  $\Delta R_s$  changes by  $\sim 21 \text{ nm}$  for  $l_p = 70 \text{ nm}$ , which roughly coincides with the value extracted by fitting the theory to experimental data. Higher (smaller) values of  $\Delta R_s$  may be obtained using larger (smaller) values of  $l_p^{CC}$  (see section III in the SI). Fig.5b, shows the distributions,  $P(R_1)$  and  $P(R_2)$  obtained from multiple trajectories as condensin undergoes a transition between the O and B states. The distributions are broad suggestive of high degree of heterogeneity.

ity in the structural transition. The large dispersion in  $P(R_1)$  and  $P(R_2)$  found in the simulations is in agreement with experiments [19], which report that the distance between the peaks is  $\Delta = 17 \pm 7$  nm whereas we find that it is  $21 \pm 7$  nm where uncertainty is calculated using standard deviation of the distributions. In the SI we show that  $\Delta R_s$  depends on the value of  $l_p^{CC}$  of the isolated Smc2 or Smc4 (Fig.1). Note that  $l_p^{CC}$  cannot be too small because a minimum rigidity in the elements transmitting allosteric signals is required [32]. Overall the simulations not only clarify the physical basis of the theory but also lend support to recent single molecule experiments [19] on a single condensin extruding loops in DNA.

In summary, we have created a theory that quantitatively explains the experimental data on a single condensin mediated loop extrusion, which is a major event in compacting chromosomes. A key prediction of our theory is that during the reaction cycle there is an allosteric transition that changes the hinge-head distance by about  $\Delta R \sim 26$  nm, which is realized if the persistence length of the isolated kinked CC exceeds  $\sim 70$  nm. We conclude with a few additional remarks. (1) We focused only on one-sided loop extrusion (asymmetric process) scenario for a single condensin, as demonstrated in the *in vitro* ex-

periment [8]. Whether symmetric LE could occur when more than one condensin loads onto DNA producing Z-loop structures [13] and if the LE mechanism depends on the species [33] is yet to be settled. Similar issues likely exist in loop extrusion mediated by cohesins [14, 34]. We believe that our work, which only relies on the polymer characteristics of DNA and implicitly on an allosteric mechanism for loop extrusion, provides a framework for theoretical investigation of LE by different scenarios. (2) If our estimate that 76 bps ( $\Delta R \approx 26$  nm) is taken literally, the theoretical value of the ideal stall force would be,  $f_{max} \approx \frac{\mu - W_{bend}}{\Delta R}$ . A naive estimate yields  $f_{max} \approx 3$  pN, exceeding 1 pN (see Fig.S7 in the SI), which implies that SMC complexes are inefficient motors. (3) Finally, if LE occurs by scrunching, as gleaned from simulations, and advocated through experimental studies [19], it implies that the location of the motor is relatively fixed on the DNA and the loop is extruded by transitions that occur in the coiled coils.

**Acknowledgements:** We thank Rasika Harshey, Changbong Hyeon, and Mauro Mugnai for useful comments. This work was supported by NSF (CHE 19-00093), NIH (GM - 107703) and the Welch Foundation Grant F-0019 through the Collie-Welch chair.

---

[1] W. Flemming, *Zellsubstanz, kern und zelltheilung* (Vogel, 1882).

[2] B. Alberts, D. Bray, K. Hopkin, A. D. Johnson, J. Lewis, M. Raff, K. Roberts, and P. Walter, *Essential cell biology* (Garland Science, 2013).

[3] K. A. Hagstrom and B. J. Meyer, *Nature Reviews Genetics* **4**, 520 (2003).

[4] S. Yatskevich, J. Rhodes, and K. Nasmyth, *Annual Review of Genetics* **53**, 445 (2019).

[5] K. Nasmyth, *Annual review of genetics* **35**, 673 (2001).

[6] G. Fudenberg, M. Imakaev, C. Lu, A. Goloborodko, N. Abdennur, and L. A. Mirny, *Cell reports* **15**, 2038 (2016).

[7] T. Terakawa, S. Bisht, J. M. Eeftens, C. Dekker, C. H. Haering, and E. C. Greene, *Science* **358**, 672 (2017).

[8] M. Ganji, I. A. Shaltiel, S. Bisht, E. Kim, A. Kalichava, C. H. Haering, and C. Dekker, *Science* **360**, 102 (2018).

[9] M.-L. Diebold-Durand, H. Lee, L. B. R. Avila, H. Noh, H.-C. Shin, H. Im, F. P. Bock, F. Bürmann, A. Durand, A. Basfeld, *et al.*, *Molecular cell* **67**, 334 (2017).

[10] F. Buermann, B.-G. Lee, T. Than, L. Sinn, F. J. O'Reilly, S. Yatskevich, J. Rappaport, B. Hu, K. Nasmyth, and J. Löwe, *Nature structural & molecular biology* **26**, 227 (2019).

[11] E. Alipour and J. F. Marko, *Nucleic acids research* **40**, 11202 (2012).

[12] A. Goloborodko, M. V. Imakaev, J. F. Marko, and L. Mirny, *Elife* **5**, e14864 (2016).

[13] E. Kim, J. Kerssemakers, I. Shaltiel, C. Haering, and C. Dekker, *Biophysical Journal* **118**, 380a (2020).

[14] Y. Kim, Z. Shi, H. Zhang, I. J. Finkelstein, and H. Yu, *Science* **366**, 1345 (2019).

[15] E. J. Banigan and L. A. Mirny, *Physical Review X* **9**, 031007 (2019).

[16] J. F. Marko, P. De Los Rios, A. Barducci, and S. Gruber, *Nucleic acids research* **47**, 6956 (2019).

[17] A. N. Kapanidis, E. Margeat, S. O. Ho, E. Kortkhonja, S. Weiss, and R. H. Ebright, *Science* **314**, 1144 (2006).

[18] J. Chen, S. A. Darst, and D. Thirumalai, *Proceedings of the National Academy of Sciences* **107**, 12523 (2010).

[19] J.-K. Ryu, A. J. Katan, E. O. van der Sluis, T. Wisse, R. de Groot, C. Hearing, and C. Dekker, *bioRxiv* (2019).

[20] J. Lawrimore, B. Friedman, A. Doshi, and K. Bloom, in *Cold Spring Harbor symposia on quantitative biology*, Vol. 82 (Cold Spring Harbor Laboratory Press, 2017) pp. 101–109.

[21] J. Wilhelm and W. Frey, *Phys. Rev. Lett.* **77**, 2581 (1996).

[22] J. Bhattacharjee, D. Thirumalai, and J. Bryngelson, *arXiv preprint cond-mat/9709345* (1997).

[23] C. Hyeon and D. Thirumalai, *The Journal of chemical physics* **124**, 104905 (2006).

[24] D. Thirumalai, *The Journal of Physical Chemistry B* **103**, 608 (1999).

[25] U. Seifert, *EPL (Europhysics Letters)* **70**, 36 (2005).

[26] U. Seifert, *Reports on progress in physics* **75**, 126001 (2012).

[27] M. L. Mugnai, C. Hyeon, M. Hinczewski, and D. Thirumalai, *Reviews of Modern Physics* **92**, 025001 (2020).

[28] J. F. Marko and E. D. Siggia, *Macromolecules* **28**, 8759 (1995).

[29] M. Rubinstein, R. H. Colby, *et al.*, *Polymer physics*, Vol. 23 (Oxford university press New York, 2003).

[30] J. M. Eeftens, A. J. Katan, M. Kschonsak, M. Hassler,

L. de Wilde, E. M. Dief, C. H. Haering, and C. Dekker, *Cell reports* **14**, 1813 (2016).

[31] M. Hinczewski, R. Tehver, and D. Thirumalai, *Proceedings of the National Academy of Sciences* **110**, E4059 (2013).

[32] D. Thirumalai, C. Hyeon, P. I. Zhuravlev, and G. H. Lorimer, *Chemical reviews* **119**, 6788 (2019).

[33] M. Kong, E. Cutts, D. Pan, F. Beuron, T. Kaliyappan, C. Xue, E. Morris, A. Musacchio, A. Vannini, and E. C. Greene, *bioRxiv* , 683540 (2019).

[34] I. F. Davidson, B. Bauer, D. Goetz, W. Tang, G. Wutz, and J.-M. Peters, *Science* **366**, 1338 (2019).

## Supplementary Information

### On the theory of condensin mediated loop extrusion in genomes

Ryota Takaki

*Physics Department, The university of Texas at Austin*

Atreya Dey, Guang Shi, and D. Thirumalai

*Chemistry Department, The university of Texas at Austin*

(Dated: January 20, 2022)

## CONTENTS

I. Simulations	3
A. Model for Condensin	3
B. Energy function	5
II. Persistence length of the Coiled-coil	6
III. Distribution of head-hinge distance	7
IV. Condensin Power Stroke	9
V. Derivation of $P(\mathcal{L} \mathcal{R})$	10
VI. Load dependence of LE velocity	11
VII. Effect of variable persistence length for DNA	12
References	14

## I. SIMULATIONS

The purpose of the simulations is to show that the extracted parameter values by fitting the theoretical extrusion rate or equivalently the velocity of loop extrusion (LE) to experiments are reasonable. In particular, we use simulations to argue that the value of  $\Delta R \approx 26$  nm (see the main text for details) is consistent with the known condensin architecture. To this end, we imagine that during the ATPase cycle the SMC motor undergoes a conformational change from a "open" (top structure in Fig. S1) to a "closed" (bottom structure) state, which brings the motor domains close to the hinge region. This process is allosterically driven, in a manner similar to other cargo-carrying motors (myosins, kinesins and dynein), by binding and hydrolysis of ATP. We envision that in the SMC the allosteric transitions are effectuated through the movement of the flexible elbow region.

### A. Model for Condensin

We modeled the two heads of condensin as spheres that are connected by finitely-extensible nonlinear elastic (FENE) potential [1] to the coiled coils (CCs) that connect the motor domains to the hinge (Fig.S1). The CC in the SMCs are reminiscent of the lever arm in Myosin V. The angle  $\theta_1$  and  $\theta_2$  are formed at the junctions connecting the motor heads to the first bead on the CCs (Fig.S1). As in molecular motors, a change in the conformation change initiated in the head domain is somewhat amplified over condensin through the CCs. We envision this process as the principle mechanism by which a spool (roughly  $\frac{\Delta R}{0.34} = 76$  base pairs (bps) in a single step) of dsDNA could be extruded.

We used 19 and 18 beads for upper CC and lower CC, respectively. The diameter of each bead is 1 nm diameter each. We used 3 beads (diameter 0.4 nm each) in the middle of the CCs for the elbow region. The angle potential in the elbow region, marking the break in an otherwise stiff CC, is sufficiently weak to facilitate the allosteric propagation of conformational changes in the motor head. For the hinge and two motor heads we used 4 nm diameter beads.

All lengths are measured in units of  $\sigma = 1$  nm corresponding to the diameter of the beads in the CC. We express energy in the unit of  $k_B T$ , where  $k_B$  is the Boltzmann constant and  $T$  is the temperature. The mass of all the particles were set to  $m = 1$ . We performed

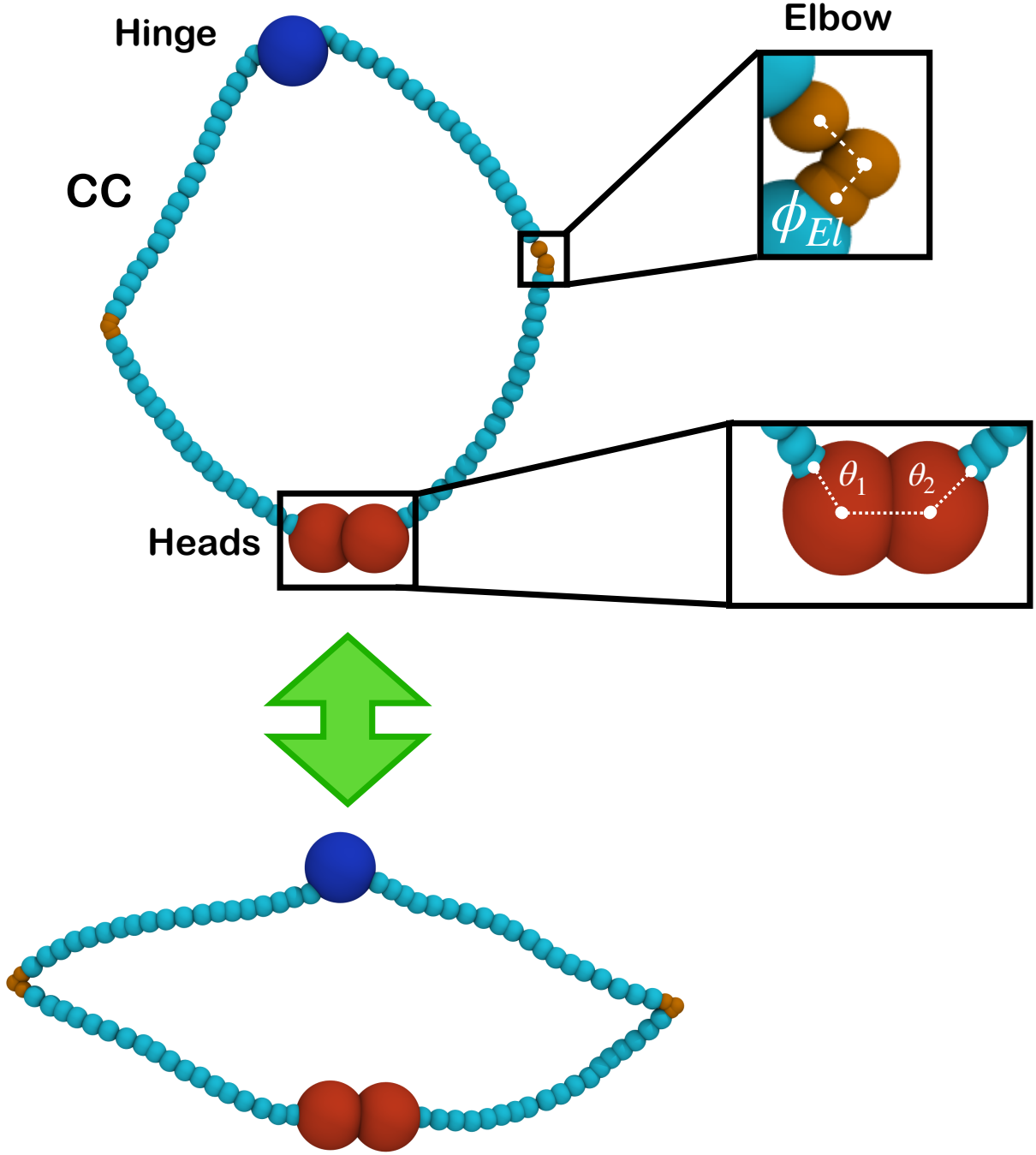


FIG. S1. Caricature of the condensin motor, an example of the Structural Maintenance of Chromosomes (SMC), used in the simulations. The two heads are shown as red spheres. A magnified image of the angle between the motor heads at the junctions to the two arms of the SMC are shown in the lower box. The angle at the elbow is depicted in the upper box. The coiled coils (CCs) connecting the motor to the hinge (purple sphere) are treated as a semi-flexible polymers that are kinked at the flexible elbow region. We envision that the allosteric transition between the open and the closed states (shown as by the green arrow) is driven by ATP binding and hydrolysis to the motor domains.

low-friction Langevin dynamics simulations using OpenMM [2] software using a time-step of  $\Delta t_L = 0.01\tau_L$ , where  $\tau_L = 0.4\sqrt{m\sigma^2/k_B T}$ . The value of the friction coefficient is  $0.01/\tau_L$ . The friction coefficient was chosen to be as low as possible for a stable simulation.

## B. Energy function

Because the goal is to merely illustrate that the hypothesized allosteric mechanism for SMC-mediated LE is plausible, we chose a simple energy function to monitor the conformational changes in condensin. The explicit form of the energy function is,

$$E(\vec{r}_1, \vec{r}_2, \dots, \vec{r}_N, \vec{\phi}, \vec{\theta}) = \sum_{i=1}^{N-1} U_{FENE}(r_{i,i+1}) + \sum_{i \neq j}^N U_N(r_{i,j}) + \left( \sum_{i \in CC \neq El} U_{ANG}^{CC}(\phi_i) + \sum_{i \in El} U_{ANG}^{El}(\phi_i) \right) + \sum_{i \in Head} U_{CNF}(\theta_i). \quad (S1)$$

The first term in Eq. S1 enforces the connectivity of the beads and is given by,

$$U_{FENE}(r_{i,i+1}) = -\frac{1}{2}k_F R_F^2 \log \left[ 1 - \frac{(r_{i,i+1} - r_{i,i+1}^0)^2}{R_F^2} \right], \quad (S2)$$

where  $k_F$  is the stiffness of the potential,  $R_F$  is the upper bound for the displacement, and  $r_{i,i+1}^0$  is the equilibrium distance between the beads,  $i$  and  $i + 1$ . The second term in Eq.S1, accounting for excluded volume interactions, is given by,

$$U_N(r_{i,j}) = \epsilon_N \left( \frac{\sigma}{r_{i,j}} \right)^{12}, \quad (S3)$$

where  $\epsilon_N$  and  $\sigma$  are the strength and range of the interaction, respectively. We used additive interactions, which means that  $\sigma$  is the sum of the radii of the two interacting beads. The third and the fourth terms in Eq.S1 are the two angle potentials that control the bending stiffness of the CCs. The potential  $U_{ANG}(\phi_i)$  is taken to be,

$$U_{ANG}(\phi_i) = \epsilon_b (1 + \cos \phi_i), \quad (S4)$$

Parameter	Value
$k_F$	$50(k_B T/\text{nm}^2)$
$R_F$	$1.5(\text{nm})$
$\epsilon_b^{CC}$	$4, 15, 30, 45, 60, 75, 90, 105, 120, 135, 150(k_B T)$
$\epsilon_b^{El}$	$4(k_B T)$
$\epsilon_N$	$5(k_B T)$
$k_C$	$100(k_B T/\text{rad}^2)$

TABLE S1. Parameters for the molecular dynamics simulation.

where  $\epsilon_b$ , the energy scale for bending, is related to the persistence length of the semi-flexible CC (see Section.II). We used a different value of  $\epsilon_b$  for  $U_{ANG}^{CC}(\epsilon_b^{CC})$  and  $U_{ANG}^{El}(\epsilon_b^{El})$  to realize the difference in the stiffness between the elbow region, and the rest of the CC. Because the persistence of the CC,  $l_p^{CC}$ , is not known we varied  $\epsilon_b^{CC}$  to cover a range of plausible values of  $l_p^{CC}$  (see Table S1).

The last term in Eq.S1 models the conformation change in the motor head of condensin due to ATP binding, and is taken as,

$$U_{CNF}(\theta_i) = k_C(\theta_i^0 - \theta_i)^2, \quad (\text{S5})$$

where  $k_C$  is the spring constant for the potential, and  $\theta_i^0$  is the equilibrium angle for the angle potential. Before the conformational change we set  $\theta_i^0 = 2.4$  (radian) in the open state, which is roughly the angle calculated by ATP engaged state of prokaryotic SMC [3]. Because the structure for closed state is unavailable we chose  $\theta_i^0 = 4.0$  (radian) for closed state, which leads to  $\theta_i \sim \pi$  (radian) in equilibrium configuration for condensin (see Fig.S5), in order to obtain a large conformational change. The transition between the open and closed states results in the scrunching of the DNA and extrusion of the loop. The parameter values in the energy function used in the simulations are in Table S1.

## II. PERSISTENCE LENGTH OF THE COILED-COIL

We calculated the persistence length ( $l_p^{CC}$ ) for coiled-coil that suffices to amplify using simulations for a single isolated semi-flexible polymer with the elbow. The single polymer

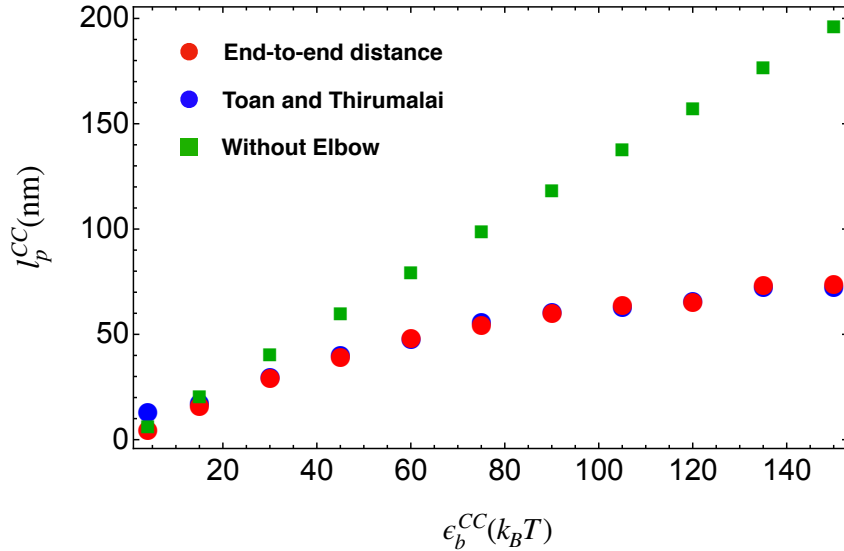


FIG. S2. Persistence length ( $l_p^{CC}$ ) as a function of bending stiffness ( $\epsilon_b^{CC}$ ). Red circles;  $l_p^{CC}$  calculated using end-to-end distance. Blue circles;  $l_p^{CC}$  calculated using the correlation of tangent angle used in Toan and Thirumalai [4]. Green squares are for a semi-flexible polymer *without* flexible elbow.

has 40 beads in total with 3 flexible beads, which provides a coarse-grained description of the CC for condensin (Sec.I A). We set  $\epsilon_b^{El} = 4(k_B T)$  and varied  $\epsilon_b^{CC}$  (see Table.S1). Since the CC in our model has flexible kink at the elbow, we computed the effective persistence length using end-to-end distance of the semi-flexible polymer. Namely, we obtained contour length ( $L$ ) and end-to-end distance ( $R$ ) from simulations then numerically solved  $\langle R^2 \rangle = 2l_p L \left(1 - \frac{l_p}{L} (1 - e^{-l_p/l_p})\right)$  [5] for  $l_p$ . We also computed the persistence length from the decay of tangent angle correlation used previously in simulating a model for DNA [4]. We found that the two methods give consistent value of effective persistence length (see Fig.S2).

Fig.S2 shows the persistence length of the CC as a function of  $\epsilon_b^{CC}$ . Without the flexible elbow, the persistence length is well approximated by  $l_p = l_b \epsilon_b / (k_B T)$ , where  $l_b \sim 1.3$  nm is mean bond length, as described elsewhere [6–8]. In the presence of the kink at the elbow the effective persistence length becomes shorter.

### III. DISTRIBUTION OF HEAD-HINGE DISTANCE

In Fig.5 in the main text we showed the distribution of head-hinge distance for  $l_p^{CC} \sim 70$  nm. Here we list distributions for different values of  $l_p^{CC}$  (Fig.S3). We also plot the mean

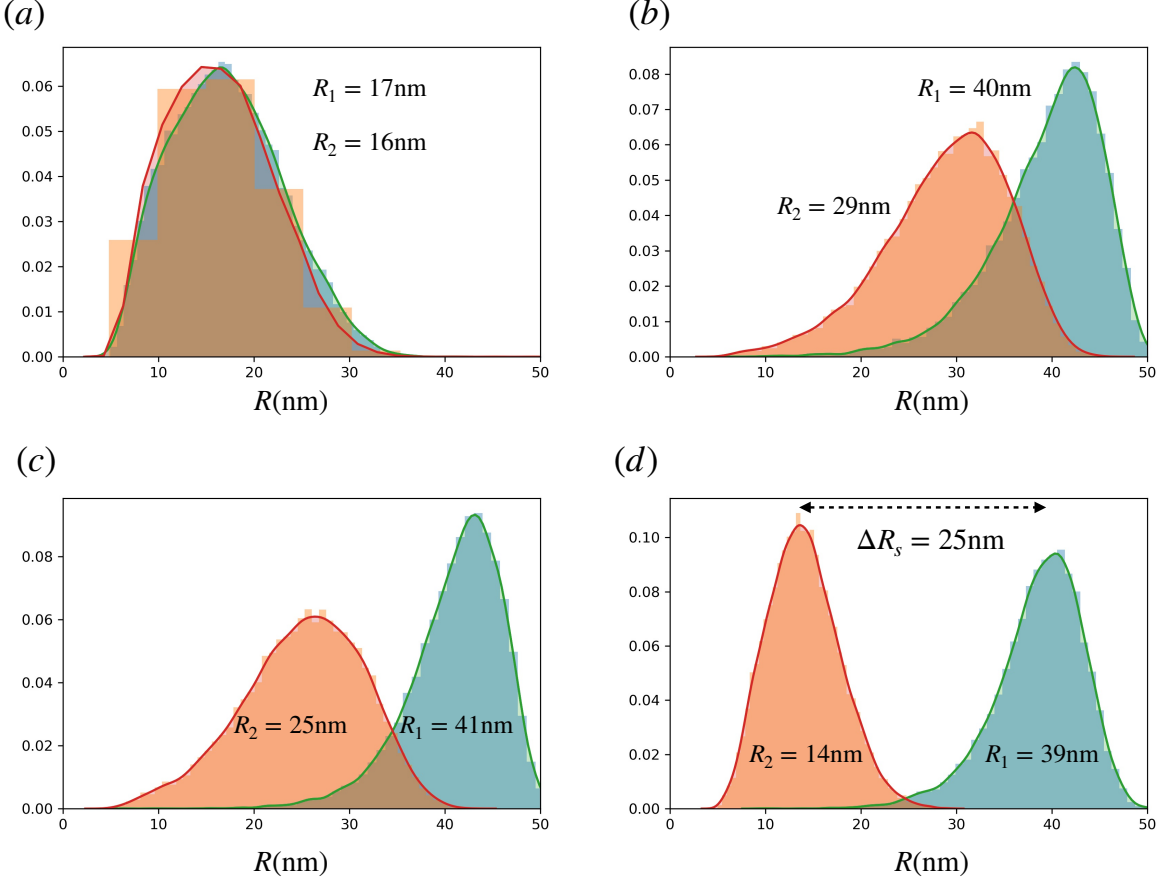


FIG. S3. Distributions of  $R$  for various  $l_p^{CC}$ .  $R_1$  and  $R_2$  are mean value of head-hinge distance for open state and closed state, respectively. The distributions are calculated from 50 trajectories, 40000 time points. (a) For  $l_p^{CC} \sim 5$  nm,  $\Delta R_s = 1 \pm 8$  nm, where error is calculated using standard deviation of the distributions. (b) For  $l_p^{CC} \sim 40$  nm,  $\Delta R_s = 11 \pm 9$  nm. (c) For  $l_p^{CC} \sim 60$  nm,  $\Delta R_s = 16 \pm 8$  nm. (d) For  $l_p^{CC} \sim 90$  nm,  $\Delta R_s = 25 \pm 6$  nm.

value of the change of head-hinge distance between open and closed state ( $\Delta R_s = R_1 - R_2$ ) as a function of  $l_p^{CC}$  (Fig.S4). For  $l_p^{CC} \sim 5$  nm (Fig.S3(a)), we find the two distributions for open state and closed state overlaps. This is because the persistence length of CC is too small to propagate the conformational change initiated at the head domain. As  $l_p^{CC}$  increases the separation of the distributions become distinct. We note that for  $l_p \sim 90$  nm,  $\Delta R_s$  reaches 25 nm, which is comparable to the conformation change estimated in our theory.

Fig.S4 shows  $\Delta R_s$  as a function of  $l_p^{CC}$ .  $\Delta R_s$  linearly increases with  $l_p^{CC}$  reaching  $\sim 25$  nm at  $l_p^{CC} \sim 90$  nm.

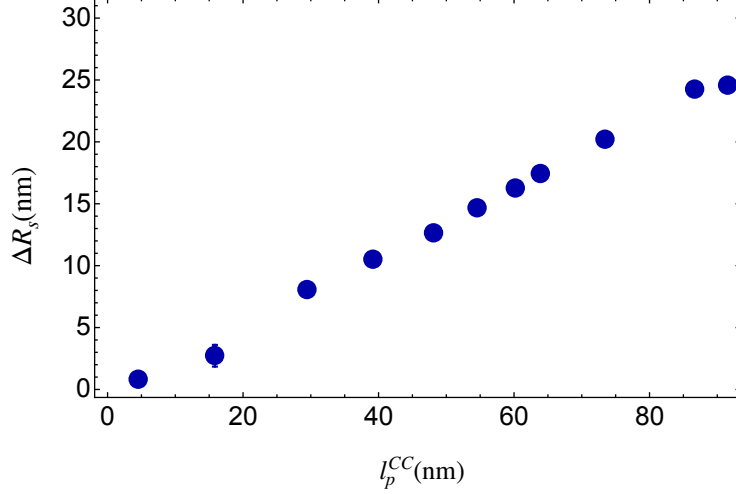


FIG. S4. Difference of head-hinge distance between open and closed state ( $\Delta R_s = R_1 - R_2$ ) as a function of  $l_p^{CC}$ . Each points are calculated from 5 trajectories (4000 time points). Error bars are mostly smaller than the plot marker.

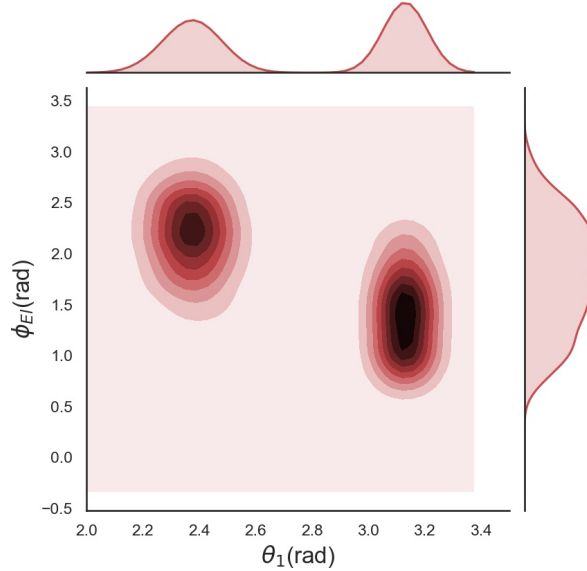


FIG. S5. Density distribution for the angles for head ( $\theta_1$ ) and for elbow ( $\phi_{El}$ ) from simulation. We plot the two dimensional distribution of angle from 50 trajectories, 40000 sample points, for  $\epsilon_b^{CC} = 150(k_B T)$  corresponding  $l_p^{CC} \sim 70$  nm. The two maximum are  $(\theta_1, \phi_{El}) = (2.4, 2.1)$  and  $(\theta_1, \phi_{El}) = (3.1, 1.4)$ . On top and the right side we show the distribution of  $\theta_1$  and  $\phi_{El}$ , respectively.

#### IV. CONDENSIN POWER STROKE

A salient feature of molecular motors is the conversion of the chemical energy released due to ATP hydrolysis to mechanical work, which is often accompanied by a power stroke

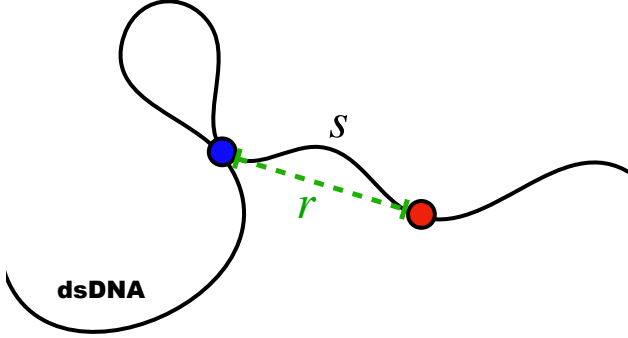


FIG. S6. A picture of a conformation of condensin bound to two loci separated by a genomic distance  $s$  (extruded loop length). The spatial distance between the attachment points in the DNA is  $r$ . For LE to occur condensin has to engage with at least two loci on the DNA.

involving conformational changes. Processive motors, such as kinesin, myosin or dynein, undergo dynamic allosteric transitions initiated by ATP binding to the motor head. We posit that a similar power stroke mechanism that produces allosteric transitions must also be operative in the SMC class of motors to translocate along the DNA, thus extruding loops. Based on AFM experiments [9, 10] and structural studies [3] we envision that open to close transition condensin (scrunching process) corresponds to condensin power stroke. The scrunching is assumed to be initiated at heads (ATPase domain), which is amplified through CC.

In the main text, we obtained head-hinge distance as a measure of the power stroke. We illustrate in Fig.S5 the distribution for the angle for the head,  $\theta_1$ , and for the elbow,  $\phi_{El}$ , (see Fig.S1 for the definition of angles) calculated from the simulation trajectories. There is a clear separation in the two dimensional distribution of the angles  $\theta_1$  and  $\phi_{El}$  (Fig.S1). The distribution of  $\theta_1$  in both the open (O shape displayed in top structure in Fig.S1) state and the closed state (B shape - a terminology used in [9] to describe the structure in the bottom of Fig.S1) is narrower than the fluctuations of  $\phi_{El}$ . Thus, even using the simple model we find that conformational changes in the head are transmitted through the elbow leading to the open to closed transition (Fig. S1).

## V. DERIVATION OF $P(\mathcal{L}|\mathcal{R})$

A major ingredient in the theory (see Eq.(1) in the main text) is the calculation of the contour length extruded loop as condensin is powered by ATP binding to the motor head and

subsequent hydrolysis. To obtain Eq.(1) in the main text let us consider condensin separated by the spatial distance  $r$  that pinches a loop whose genomic length is  $s$  (Fig.S6). Given the distribution of the spatial distance  $r$  between two loci separated by a linear genomic distance  $s$ ,  $P(r|s)$ , we would like to derive the distribution of  $s$   $P(s|r)$ . Indeed,  $P(s|r)$  is the probability of extruded length of dsDNA,  $s$  by condensin whose DNA binding domains are separated by the distance,  $r$ . According to the Bayes's rule, we have  $P(r|s)P(s) = P(s|r)P(r)$ . The normalization dictates that  $P(r) = \int_0^L P(r|s)P(s)ds$ . These two equations lead to,

$$P(s|r) = \frac{P(r|s)P(s)}{\int_0^L P(r|s)P(s)ds}.$$

We assume that there is no preference for picking any specific genomic distance  $s$  on DNA (we do not account for sequence specific preference). Consequently, we take  $P(s) = 1/L$ . Therefore,

$$\begin{aligned} P(s|r) &= \frac{(1/L)P(r|s)}{(1/L) \int_0^L P(r|s)ds} \\ &= \frac{P(r|s)}{\int_0^L P(r|s)ds}. \end{aligned}$$

Thus,  $P(s|r)$  and  $P(r|s)$  differ only by a constant,  $\int_0^L P(r|s)ds$ , if we consider a fixed  $r$ . It is clear that  $P(r|s)$  is the radial probability density for the interior segments separated by a distance  $r$  for a semi-flexible polymer, which is derived elsewhere [11]. For the case  $s = L$ ,  $P(r|s)$  is the result for the end-to-end distribution for semi-flexible chains,  $P(\mathcal{R}|\mathcal{L})$  [12]. It is known that the simple analytic result for  $P(\mathcal{R}|\mathcal{L})$  [12] is accurate when compared to the exact result [13] or numerical simulations. Thus, we employ the simpler expression  $P(\mathcal{R}|\mathcal{L})$  and assume that  $P(\mathcal{L}|\mathcal{R})$  is equivalent to  $P(\mathcal{R}|\mathcal{L})$  up to a normalization constant when expressed in terms of  $L$  with fixed  $R$ .

## VI. LOAD DEPENDENCE OF LE VELOCITY

In the experiment [14] the load acting on condensin is obtained indirectly using relative extension of dsDNA. However, in principle, it is possible to measure the direct load depen-

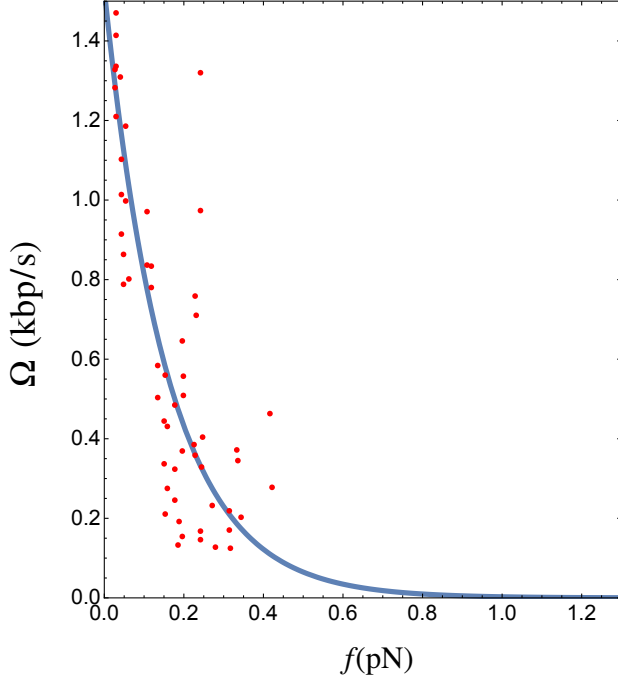


FIG. S7. Comparison of the velocity of LE predicted by theory (blue line) with the data (red dots) extracted from experiment [14].

dence of condensin by using a different experimental set up such as optical tweezers. We plotted using Eq.(4) in the main text, the LE velocity, directly as a function of external load  $f$  in Fig.S7. We also converted the experimental data from  $x$  to  $f$  using Eq.(5) in the main text. It is evident from Fig.S7 that condensin is a weak motor with a high response to the external load. Note that the rate of extrusion significantly drops by  $f = 0.4$  pN, which is consistent with previous experiments [15–17]. It appears that the stall force is no more than about  $f_s = 1.0$  pN.

## VII. EFFECT OF VARIABLE PERSISTENCE LENGTH FOR DNA

In the main text we used  $l_p = 50$  nm as the persistence length of DNA, which is widely accepted value for dsDNA [18]. However, it could be interesting to explore  $l_p$ , which can be drastically altered in the presence of divalent cations, as a variable in our theory. In Fig.S8(a) we plotted  $P(\mathcal{L}|R = 50$  nm) using Eq.(1) in the main text for different  $l_p$ . As dsDNA become flexible the distribution of  $P(\mathcal{L}|R = 50$  nm) becomes wider, suggesting that most probable value of captured length of DNA by condensin would be larger with a large dispersion. Thus, in this situation our approximation,  $\Delta l \approx \Delta R$ , would become less

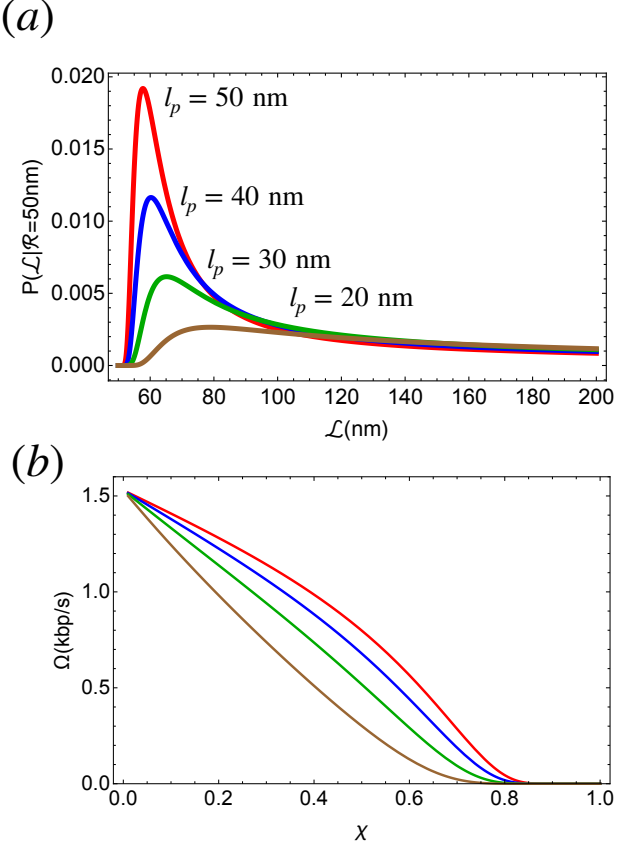


FIG. S8. Effect of variable persistence length for dsDNA. (a) Plot of  $P(L|R = 50\text{ nm})$ .  $l_p = 50\text{ nm}$  (red),  $l_p = 40\text{ nm}$  (blue),  $l_p = 30\text{ nm}$  (green), and  $l_p = 20\text{ nm}$  (brown). (b) Extrusion rate of DNA for different  $l_p$ .  $l_p = 50\text{ nm}$  (red),  $l_p = 40\text{ nm}$  (blue),  $l_p = 30\text{ nm}$  (green), and  $l_p = 20\text{ nm}$  (brown).  $\Delta R$  is fixed to be  $26\text{ nm} \sim 76\text{ bps}$ .

accurate. Nevertheless, we can explore the velocity of extrusion for different  $l_p$  shown in Fig.S8(b) for a fixed  $\Delta R = 26\text{ nm}$ . As  $l_p$  decreases the velocity of extrusion becomes linear and slower because the load acting on DNA is higher for smaller  $l_p$  at the same extension.

---

- [1] K. Kremer and G. S. Grest, *The Journal of Chemical Physics* **94**, 4103 (1991).
- [2] P. Eastman, J. Swails, J. D. Chodera, R. T. McGibbon, Y. Zhao, K. A. Beauchamp, L.-P. Wang, A. C. Simmonett, M. P. Harrigan, C. D. Stern, *et al.*, *PLoS computational biology* **13**, e1005659 (2017).
- [3] M.-L. Diebold-Durand, H. Lee, L. B. R. Avila, H. Noh, H.-C. Shin, H. Im, F. P. Bock, F. Bürmann, A. Durand, A. Basfeld, *et al.*, *Molecular cell* **67**, 334 (2017).
- [4] N. M. Toan and D. Thirumalai, *The Journal of chemical physics* **136**, 06B612 (2012).
- [5] O. Kratky and G. Porod, *Recueil des Travaux Chimiques des Pays-Bas* **68**, 1106 (1949).
- [6] Z. Benková, L. Rišpanová, and P. Cifra, *Polymers* **9**, 313 (2017).
- [7] X. Li, C. M. Schroeder, and K. D. Dorfman, *Soft Matter* **11**, 5947 (2015).
- [8] J. Midya, S. A. Egorov, K. Binder, and A. Nikoubashman, *The Journal of chemical physics* **151**, 034902 (2019).
- [9] J. M. Eeftens, A. J. Katan, M. Kschonsak, M. Hassler, L. de Wilde, E. M. Dief, C. H. Haering, and C. Dekker, *Cell reports* **14**, 1813 (2016).
- [10] J.-K. Ryu, A. J. Katan, E. O. van der Sluis, T. Wisse, R. de Groot, C. Hearing, and C. Dekker, *bioRxiv* (2019).
- [11] C. Hyeon and D. Thirumalai, *The Journal of chemical physics* **124**, 104905 (2006).
- [12] J. Bhattacharjee, D. Thirumalai, and J. Bryngelson, *arXiv preprint cond-mat/9709345* (1997).
- [13] J. Wilhelm and W. Frey, *Phys. Rev. Lett.* **77**, 2581 (1996).
- [14] M. Ganji, I. A. Shaltiel, S. Bisht, E. Kim, A. Kalichava, C. H. Haering, and C. Dekker, *Science* **360**, 102 (2018).
- [15] J. M. Eeftens, S. Bisht, J. Kerssemakers, M. Kschonsak, C. H. Haering, and C. Dekker, *The EMBO journal* **36**, 3448 (2017).
- [16] J. Eeftens and C. Dekker, *Nature structural & molecular biology* **24**, 1012 (2017).
- [17] T. R. Strick, T. Kawaguchi, and T. Hirano, *Current biology* **14**, 874 (2004).
- [18] M. Rubinstein, R. H. Colby, *et al.*, *Polymer physics*, Vol. 23 (Oxford university press New York, 2003).